

Conducting Nanocrystal Patterns Using a Silver Organic Complex Blended with Polystyrene as e-Beam Resist

T. Bhuvana, C. Subramaniam, T. Pradeep, and G. U. Kulkarni

J. Phys. Chem. C, **2009**, 113 (17), 7038-7043 • DOI: 10.1021/jp811062m • Publication Date (Web): 02 April 2009

Downloaded from <http://pubs.acs.org> on April 23, 2009

More About This Article

Additional resources and features associated with this article are available within the HTML version:

- Supporting Information
- Access to high resolution figures
- Links to articles and content related to this article
- Copyright permission to reproduce figures and/or text from this article

[View the Full Text HTML](#)

Conducting Nanocrystal Patterns Using a Silver Organic Complex Blended with Polystyrene as e-Beam Resist

T. Bhuvana,[†] C. Subramaniam,[‡] T. Pradeep,[‡] and G. U. Kulkarni^{*†}

Chemistry and Physics of Materials Unit and DST Unit on Nanoscience, Jawaharlal Nehru Centre for Advanced Scientific Research, Jakkur P O, Bangalore 560 064, India, DST Unit on Nanoscience, Department of Chemistry and Sophisticated Analytical Instrument Facility, Indian Institute of Technology Madras, Chennai 600036, India,

Received: December 15, 2008; Revised Manuscript Received: February 23, 2009

With the intention of producing a metal composite consisting of Ag nanoparticles embedded in patterned polystyrene, silver triphenylphosphine nitrate, Ag(PPh₃)₃NO₃, was chosen as a source of Ag metal as it is soluble in toluene to form a blend with polystyrene, a well-known negative tone e-beam resist. At a constant e-beam dosage of 150 $\mu\text{C cm}^{-2}$, the patterns were produced at 5, 10, and 30 keV beam energies while varying the dwell time at a location (pixel) and the number of passes. The presence of Ag in the patterned regions was confirmed by the EDS analysis. TEM showed the formation of small Ag nanoparticles in the embedded matrix of the polymer. The reduction of Ag precursor following exposure to the e beam was monitored by XPS. UV–vis absorption studies showed a broad peak at 464 nm, typical of surface plasmon absorption by Ag nanoparticles. Confocal fluorescence studies showed the embedded Ag nanoparticles in the carbon matrix to have fluorescence property as well. C-AFM measurements have shown that the patterned blend is well conducting due to the interacting Ag nanoparticles, the resistance being two orders less compared to that of polystyrene itself. The higher the beam energy, the lower was the dwell time required to attain a conducting pattern.

Introduction

Design and synthesis of patternable nanomaterials is important to device fabrication. In this context, UV or e-beam lithography based synthesis of patterned nanomaterials for active elements is a versatile method. Metal precursors containing polymer blends are good starting materials for this purpose, as the former produces active species under the lithography beam while the latter not only works like a resist but also provides the desired matrix. One such example is the spin-coatable e-beam sensitive resist consisting of metal nitrate salts and polyvinyl alcohol (PVA) based blend, which gave rise to La_{0.7}Sr_{0.3}MnO₃ patterns.¹ With regard to metal systems, Abargues et al.² reported a high-resolution negative-tone nanocomposite resist based on PVA where Ag nanoparticles and nanopatterns were simultaneously generated by the e-beam lithography. Such metal–polymer patterns may find applications in nanocircuitry and plasmonic devices. We have been interested in developing precursors for direct write lithography³ and in this article, we explore the reduction of an Ag salt in polystyrene matrix upon exposure to the e-beam, the polymer itself known to be a negative tone resist.⁴

There are many reports on polymer blends embedded with Ag nanoparticles, though not directly related to lithography. Bogle et al.⁵ reported the synthesis of Ag nanoparticles by irradiating a solution of AgNO₃ and PVA, with 6 MeV electrons whereas Mahapatra et al.⁶ used a mixture of PVA with Au and Ag metal precursors and obtained respective metal nanoparticles by exposure to a broad e-beam of 5–15 keV. Eilers et al.⁷

obtained Teflon-Ag nanocomposite by thermal evaporation of Teflon and Ag foil on sapphire substrate and found the broadening of optical absorption indicating the formation of the blend. Porel et al.⁸ have synthesized Ag and Au nanoparticles in polyvinyl alcohol (PVA) matrix by heating a mixture of the metal salt and PVA and investigated the optical limiting capability of these nanoparticle-embedded polymer blends. There are other studies where the blend contained well-known resists such as poly(methylmethacrylate) (PMMA), although no patterning was attempted. Deshmukh and Composto⁹ showed that the thermal decomposition of Ag precursor with PMMA at 185 °C leads to the formation of Ag nanoparticles and their enrichment at the surface. Basak et al.^{10,11} have studied the photoluminescence and electrical conductivity of thin films of PMMA dispersed with Ag nanoparticles. The authors showed that the electrical conduction was caused by the conducting paths established through the proximal interaction between neighboring nanoparticles.

In this article, we report our investigations on a blend of Ag(PPh₃)₃NO₃–polystyrene used as a e-beam resist for patterning. Our intention was to exploit the e-resist behavior of polystyrene and doping it with metallic Ag species to improve its electrical conduction behavior and thus produce conducting patterns. We have carried out detailed characterization of the written patterns using X-ray photoelectron spectroscopy (XPS), transmission electron (TEM), and scanning transmission (STEM) microscopy as well as confocal fluorescence and Raman spectroscopy. Further, we have examined the electrical conduction behavior of the written patterns using conducting-AFM (C-AFM). Our results have shown that moderate e-beam exposures convert the resist blend into patterns filled with Ag nanocrystals in carbon matrix with good electrical conduction property.

* To whom correspondence should be addressed. E-mail: kulkarni@jncasr.ac.in. Fax: +91-80-22082766.

[†] Jawaharlal Nehru Centre for Advanced Scientific Research.

[‡] Indian Institute of Technology Madras.

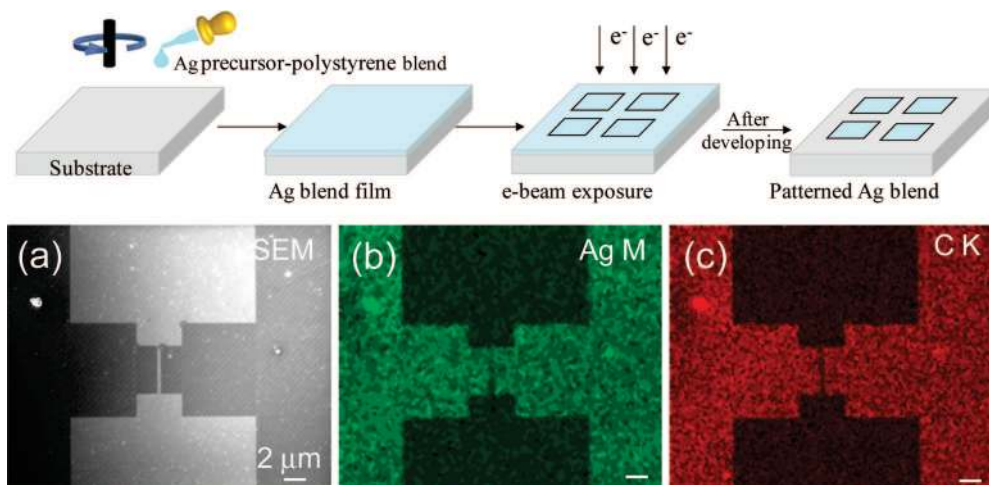


Figure 1. Schematic showing the procedure adopted for patterning Ag precursor-polystyrene blend using EBL. Step 1: Spin coating of $\text{Ag}(\text{PPh}_3)_3\text{NO}_3$ -polystyrene blend on a Si substrate. Step 2: EBL patterning and Step 3: Developing the patterned substrate in *p*-xylene and 2-propanol for 90 and 30 s, respectively. (a) SEM image of a patterned gap electrode. EDS maps obtained using (b) Ag M and (c) C K lines.

Experimental Section

The Ag precursor, namely its triphenylphosphine nitrate ($\text{Ag}(\text{PPh}_3)_3\text{NO}_3$) was prepared following a literature procedure.¹² In order to perform e-beam lithography, the resist was prepared by blending a saturated solution of the Ag precursor in toluene with commercially available polystyrene ($M_w = 260\,000$) such that the resulting solution had 1 wt % of polystyrene. This blend was spin-coated at 3000 rpm on clean Si, SiO_2/Si , and ITO substrates. Electron beam lithography (EBL), was performed on the blend film coated on a Si substrate using an e-beam writer available with Nova NanoSEM 600 equipment (FEI Co., The Netherlands). An array of $8 \times 8 \mu\text{m}^2$ square regions was exposed to e-dosage of $150 \mu\text{C cm}^{-2}$ at different beam energies 5–30 kV. For the negative tone behavior of polystyrene, this dosage is adequate.¹³ Electron exposure was carried out with constant e-dosage while varying internal parameters such as the dwell time and number of passes. The substrate was then developed in *p*-xylene and 2-propanol for 90 and 30 s, respectively, as is usually done for polystyrene.¹⁴ Further, the patterned substrate was dried under flowing nitrogen. The procedure is shown in the scheme in Figure 1. For a $60 \mu\text{L}$ of the blend, the pattern thickness achieved was typically 180 nm, as revealed in the step measurements using an optical profilometer (NT1100, Wyko, Veeco Instruments, USA).

Energy dispersive spectroscopy (EDS) analysis was performed at 10 kV (energy window, 10 eV) with a beam current of 1.1 nA, the dwell time per pixel being $30 \mu\text{s}$ using an EDAX Genesis (Mahwah, USA), attached to the SEM column. STEM (scanning transmission electron microscopy) was also performed using the same equipment. UV–visible spectra were recorded using a Perkin–Elmer Lambda 900 UV/vis/NIR spectrophotometer. The core-level Ag(3d) spectra were measured using a VG scientific ESCALAB MK-IV spectrophotometer with an X-ray source of Al $K\alpha$ (1486.6 eV). In order to perform transmission electron microscopy (TEM), a holey carbon grid was drop coated with the blend and patterned. High-resolution TEM imaging was carried out with a JEOL-3010 equipment operating at 300 kV. C-AFM measurements using Au coated tips¹⁵ were performed on patterned ITO substrate employing a Digital Instruments Multimode head attached to a Nanoscope-IV controller (Veeco, USA) and an external multimeter (Keithley 236). The Raman and fluorescence spectra were collected

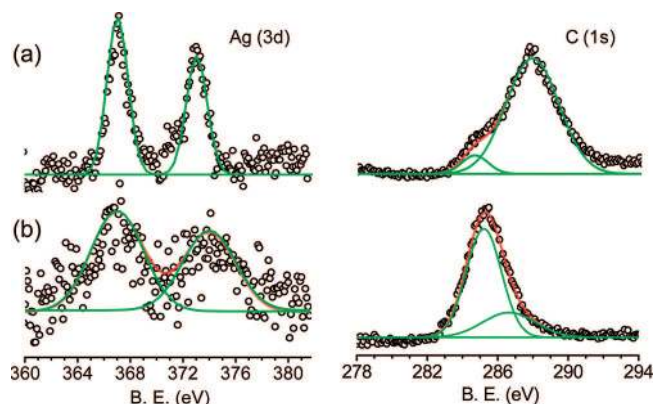


Figure 2. Ag(3d) and C(1s) core level spectra of the blend before (a) and after (b) e-beam exposure. The relatively higher spread in data points in (b) is due to poor signal strength as e-beam exposed region was limited to $3 \times 3 \mu\text{m}^2$.

using patterned ITO with 514.5 nm Ar ion laser excitation (spot size $< 1 \mu\text{m}$). The laser beam power was $\sim 15 \text{ mW}$. The backscattered light was collected using a $100\times$ objective lens and typical signal acquisition time at each pixel of the image was 0.1 s.

Results and Discussion

In Figure 1, are shown the patterns drawn using a $\text{Ag}(\text{PPh}_3)_3\text{NO}_3$ -polystyrene blend for e-beam lithography. As polystyrene is a negative-tone resist, the e-beam exposed regions get cross-linked and remain after developing while rest of the polymer gets washed away. Figure 1a shows the SEM image of a $\sim 500 \text{ nm}$ gap electrode patterned with the blend resist with an e-dose of $150 \mu\text{C cm}^{-2}$ with 5 kV. The EDS mapping at Ag M and C K lines showed clearly the presence of Ag and C in the patterned regions (Figure 1, panels b and c). The roughness associated with the edges of the pattern was $\sim 3 \text{ nm}$ typical of polystyrene itself.¹⁶ The atomic ratio of Ag and carbon as determined by EDS was 6:94.

The effect of the e-beam exposure on the chemical nature of the blend was examined employing XPS (Figure 2). For this purpose, a large area of $3 \times 3 \mu\text{m}^2$ was patterned using 5 kV beam at $150 \mu\text{C cm}^{-2}$. We show the Ag(3d) and C(1s) core-level spectra before and after e-beam exposure in Figure 2,

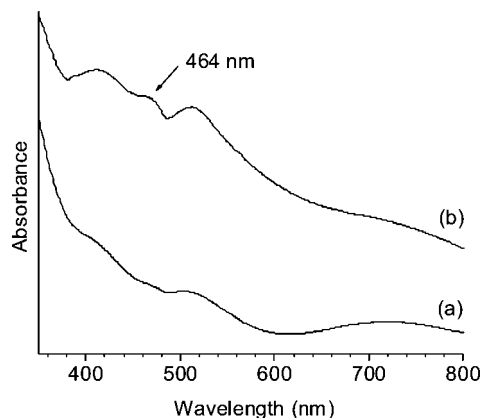


Figure 3. Optical absorption spectra of the blend (a) before and (b) after e-dosage. The feature marked with an arrow represents surface plasmon absorption from Ag nanoparticles.

panels a and b, respectively. Prior to e-beam exposure, the Ag(3d) spin-orbit doublets are observed at 367.2 and 373.1 eV (Figure 2a) and after e-dosage, at 367.0 and 373.9 eV (Figure 2b) and the area under the curves being nearly same. Ag(3d) peak became broad and shifted slightly to a lower binding energy. Considering Ag(3d) shows only a small shift from Ag⁺ to Ag⁰ (~0.3 eV),¹⁷ the above observation is taken to indicate the reduction of the Ag complex. The C(1s) region, prior to exposure (Figure 2a) was found to contain two features at 284.6 and 287.8 eV due to graphitic and sp³ carbon respectively, whereas after e-beam exposure (Figure 2b), the main peak position shifted to 285.3 and with a lower intensity peak at 286.6 eV. The shift to a lower binding energy is taken to indicate the formation of more graphitic carbon in comparison to hydrocarbon before exposure to e-beam.

From XPS studies, it is clear that the reduction of Ag species takes place upon exposure to e-beam. This has been further confirmed by UV-vis absorption measurements as shown in Figure 3. The surface plasmon peak at 464 nm for the e-dosed sample (spectrum b) is clear indication for the formation of Ag nanoparticles^{7,18} which is absent in the case of unexposed blend (spectrum a). This peak is red-shifted with respect to colloidal Ag, which is typically 420 nm.¹⁹ Such a red-shift is expected in a mesoscale assembly due to proximal electronic coupling among neighboring particles.²⁰

TEM and STEM measurements also support the formation of Ag nanoparticles in the carbon matrix as shown in Figure 4. TEM image of the Ag nanoparticles sized 20–50 nm in the carbon matrix is shown in Figure 4a. High-resolution imaging in the top inset shows dark features corresponding to metal nanoparticles of 3–5 nm diameter. It appears that the big features seen at lower magnifications are indeed made up of such finer particles. Electron diffraction pattern in the bottom inset clearly shows sharp spots corresponding to (111) and (200) diffraction planes, implying good crystallinity of the Ag nanoparticles. STEM image shown in Figure 4b brings out particulate arrangement within an aggregate. Individual Ag nanoparticles and their aggregates are seen embedded in thick carbon shells. In order to further strengthen the observations, a TEM grid coated with the neat triphenylphosphine complex (without polystyrene) was exposed to the e-beam under similar conditions (150 $\mu\text{C cm}^{-2}$). TEM image in Figure 5 shows the formation of agglomerated Ag nanoparticles sized 25–35 nm. The particle size is somewhat larger than that shown in Figure 4a, as the polymer matrix is absent in this case. Electron diffraction pattern shown in the inset confirms the crystallinity

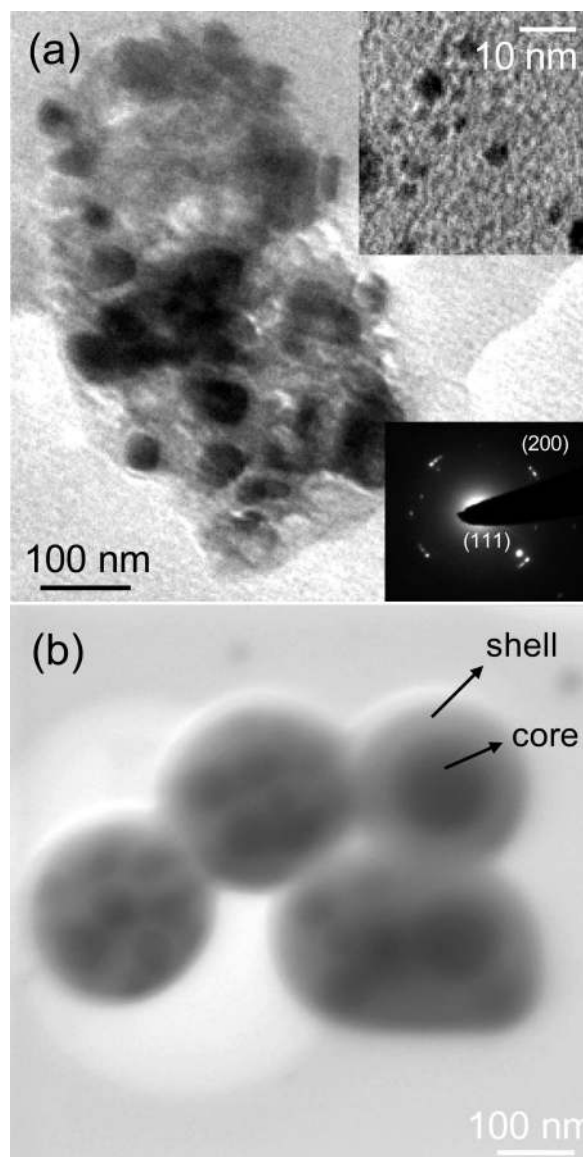


Figure 4. (a) TEM image of the e-beam exposed cross-linked blend showing formation of Ag nanoparticles. Inset showing high-resolution image (top) and corresponding electron diffraction pattern (bottom). (b) STEM image of the Ag nanoparticle aggregate. The core and shell regions are marked.

of the nanoparticles. High resolution imaging was not possible due to interference from the organic ligands adsorbed on the particle surface. What is noteworthy from this experiment is that the silver organic complex used in forming the resist blend undergoes facile reduction under the e beam conditions employed.

The resist blend exposed to e-beam was further examined under confocal fluorescence and Raman microscopy (Figure 6). The intensities of the desired portion of the spectra collected over all of the pixels were compared by ScanCTRL Spectroscopy Plus Version 1.32 software, to construct a color-coded image. Regions coded yellow represent the pixels where the signal (used for mapping) is maximum, the minimum being represented with red/black colors. The scattered radiation comprising of the Rayleigh is the major component. The dark regions of the sample indicate that there is absorption of the incident radiation. All other experimental parameters remained the same including the laser flux, time of exposure, accumulation time and so on. Employing the supernotch filter, we collected only the emission from the sample. The confocal (Figure 6a)

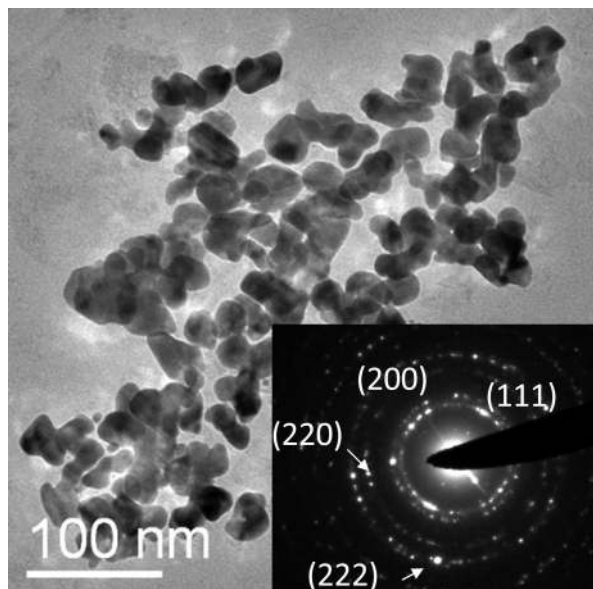


Figure 5. TEM image of the e-beam exposed Ag precursor (without polystyrene) showing the formation Ag nanoparticles with the inset containing the corresponding electron diffraction pattern.

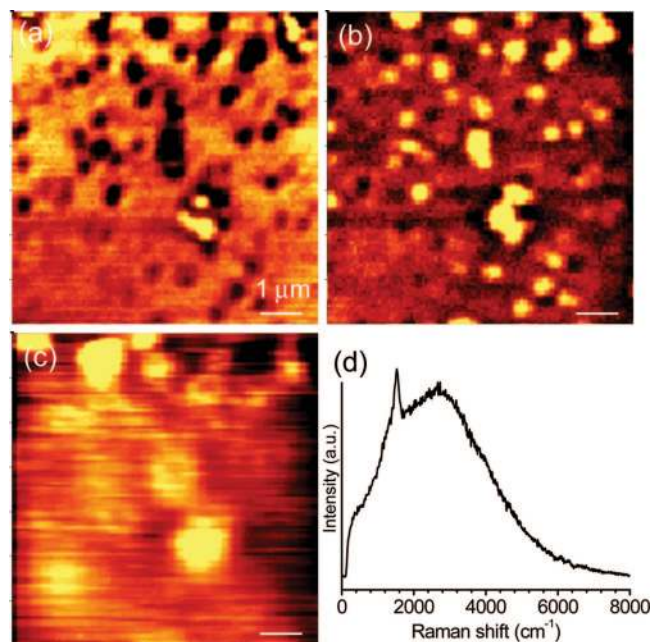


Figure 6. (a) Confocal image of Ag nanoparticles in cross-linked polystyrene matrix. Fluorescence (b) and Raman (c) images from the same region. (d) Raman spectrum from the same region. Raman image was acquired using the 1524 cm^{-1} feature. The images correspond to the same area.

and the confocal (Figure 6b) fluorescence images are complementary to each other, meaning that the regions from which the sample absorbs the excitation radiation (shown as dark regions in the confocal image) are the regions from which it emits light in the confocal fluorescence image. This may be interpreted as the absorption by the embedded Ag particles/aggregates or species at the nanoparticle surfaces and their subsequent emission. In view of the significant absorption manifested at these locations, it is likely that the black spots are due to nanoparticles, which is in agreement with the TEM and STEM investigations as shown in Figure 4. The plasmon absorption of large Ag particles/aggregates falls in the region of the excitation radiation.^{7,21} These findings may be related to

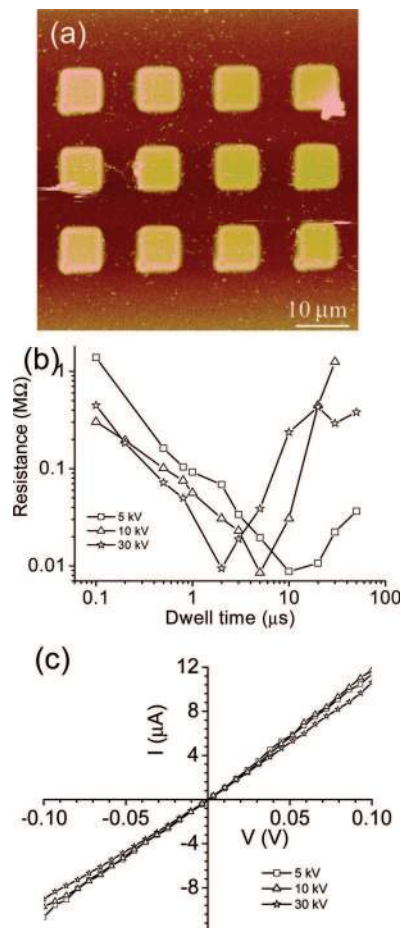


Figure 7. (a) AFM image of an array of square islands of the Ag nanoparticles polystyrene composite. (b) Plot of resistance versus dwell time for different islands patterned at 5, 10, and 30 kV. (c) I - V measurement made using C-AFM showing the lowest resistance obtained with different kVs.

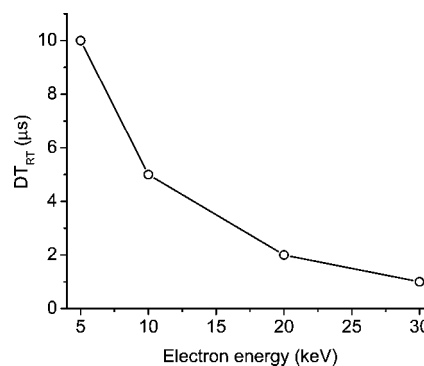


Figure 8. Plot of dwell time at which lowest resistance was observed for different kVs.

the literature. Visible emission from Ag nanoparticle–carbon nanotube composites due to nanoparticle interaction has been reported recently.²² Molecules localized between coupled Ag metal nanoparticles have been shown to exhibit enhanced fluorescence.²³ The emission spectrum collected from a spot on the sample using the Raman setup (grating, 150 grooves/mm) is given in Figure 5d. The creation of carbonaceous species by e-beam irradiation may be confirmed from the Raman peak at 1524 cm^{-1} , which is in accordance with the Raman feature of amorphous carbon.^{24,25} The Raman image accumulated riding on the 1524 cm^{-1} feature showed enhanced intensity around the regions of fluorescence suggesting that these two aspects

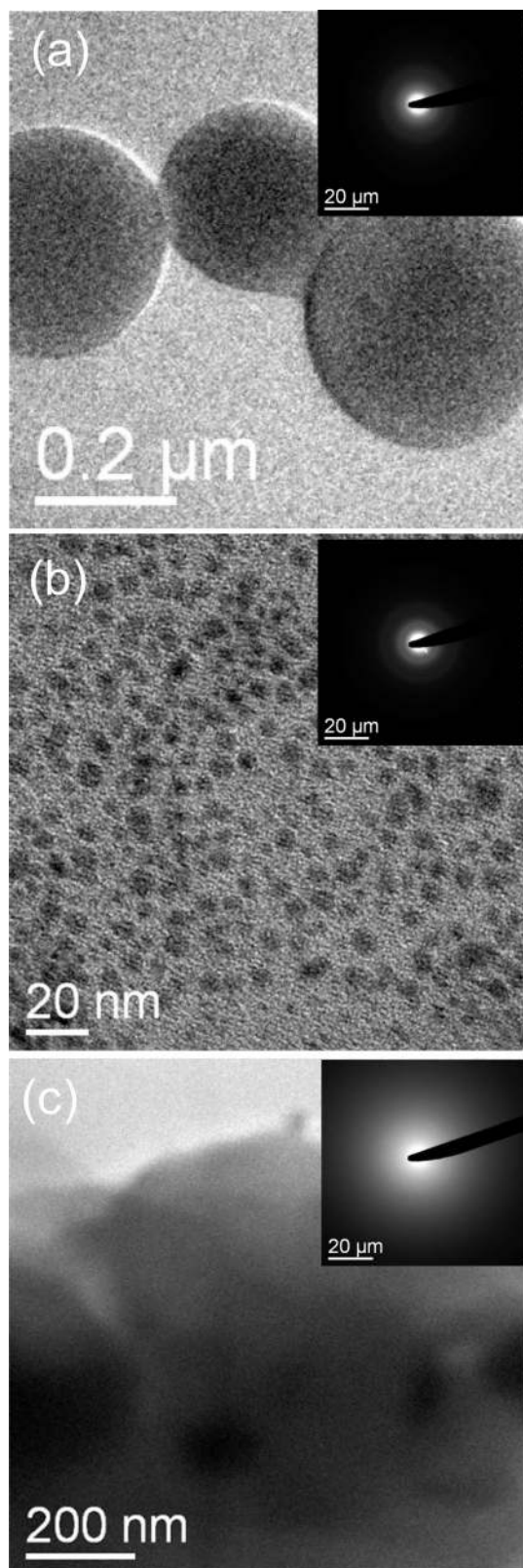


Figure 9. TEM images with corresponding ED patterns shown in the inset for patterned regions at 30 kV with different dwell times (a) 0.5, (b) 1, and 50 μs .

are related. As the 1524 cm^{-1} feature is overlapped with fluorescence and this feature can also arise from Ag-poor regions, a one-to-one correlation between panels b and c in Figure 6 cannot be made.

From the above studies, it is clear that the e-beam exposure of the resist blend brings about reduction of Ag^+ to form Ag

nanoparticles (3–5 nm) covered with a thin layer of amorphous carbon. Such core–shell particles would be good candidates for electrical transport. Previously, it is reported that Ag and Cu nanowires have low electrical percolation threshold in polystyrene composites.²⁶ In order to evaluate the conducting property, an array of 4×4 islands each of size $8 \times 8\ \mu\text{m}^2$ was patterned and C-AFM was performed on the individual islands (Figure 7). A typical AFM image is shown in Figure 7a. The islands marked 1–12 have been given a constant e-dosage of $150\ \mu\text{C cm}^{-2}$ at 5 keV while varying the dwell time (0.1–50 μs) and the number of passes (16 000–8). The e-dosage was kept constant at a moderate value ($150\ \mu\text{C cm}^{-2}$), such that the evolution of the metallic species could be studied. This exercise was repeated at e-beam energies of 10 and 30 keV. From CAFM data in Figure 7b, we see that at a given kV, the sheet resistance of the islands is in the range of M Ω s at lower dwell times (<0.2 μs). On increasing the dwell time, the resistance dropped to $\sim 8\ \text{k}\Omega$ and then increased. This trend was observed irrespective of the kV employed, with the only difference that the dwell time required to reach the lowest resistance was less, higher the e-beam energy. Independent of the e-beam energy employed, all I–V curves were linear with resistance of 8.3 k Ω (Figure 7c). On the other hand, the resistance values were at least two orders higher for pristine polystyrene patterns of similar dimensions. It appears that the electrical conduction arises due to the proximal interaction between neighboring nanoparticles similar to the situation observed earlier in the case of nanoparticles–polymer blends.^{10,11} The conduction path is set up by Ag nanoparticles giving rise to ohmic behavior in the polymeric matrix.^{10,11} Interparticle interaction giving rise to enhanced electrical conduction is common in mesoscale assemblies of metal nanoparticles.²⁰

In Figure 8, a plot of the dwell time required to attain the lowest resistance is shown for different e-beam energies. At an e-beam energy of 30 kV, it is around 1 μs per pixel, whereas for 5 kV, it is 10 μs per pixel. Thus, the higher the beam energy, the shorter the dwell time required to generate the most conducting pattern. TEM studies were carried out on the regions subjected to different dwell times at 30 kV. Figure 9a shows some evidence of the nucleation of Ag nanoparticles at a lower dwell time (0.5 μs), whereas at 1 μs , well formed Ag nanoparticles are seen in the carbon matrix (Figure 9b). The ED pattern shows distinct rings, which confirms the overall crystallinity nature of the Ag nanoparticles. Clearly, this emphasizes the observed trend in the resistance with the dwell time (Figure 9b). On further increasing the dwell time to 50 μs , TEM image obtained is almost devoid of Ag nanoparticles (Figure 9c), and the ED pattern shown in the inset appears featureless and diffused. A higher dwell time of the e beam at a given region (pixel) seems to ablate the metallic species. The effect of dwell time is evident. At a given beam energy, it requires an optimal dwell time for Ag nanoparticles to nucleate and grow. A lesser dwell time, even though it is repeated a greater number of times, proves insufficient in inducing Ag nanoparticle growth. A higher dwell time seems to take away the metallic species leaving behind only carbon-based matrix, which is less conducting.

Conclusion

Electron beam patterning of Ag, using silver triphenylphosphine mixed with a negative tone e-beam resist, namely, polystyrene, is demonstrated. On exposure to e-beam, reduction of Ag takes place resulting in a core–shell structure with carbon made available from polystyrene forming the shell. The nano-

particles are of 5–50 nm in size and form bigger aggregates. The reduction of Ag was also confirmed by XPS measurements which showed the presence of Ag⁰ peaks at 367.2 and 373.1 eV while UV–vis spectra showed a peak around 464 nm, characteristics of surface plasmon absorption of Ag nanoparticles. The Ag-carbon core shell structures exhibit fluorescence property. C-AFM studies carried out on the patterned blend supported the formation of metallised polystyrene with the resistance values two orders better than that of the pristine. Proximal electronic interaction between neighboring nanoparticles is believed to be responsible for the electrical conduction. Thus, the study has shown how conducting patterns of polystyrene can be obtained by doping with Ag nanoparticles grown in situ. The negative resist behavior of polystyrene in combination with the ability of the Ag complex to reduce under e-beam has been exploited, making the blend a potential electron resist material for conducting patterns.

Acknowledgment. The authors are grateful to Professor C. N. R. Rao for his encouragement. Financial support from the Department of Science and Technology, Government of India, is gratefully acknowledged. The authors thank Ms. B Radha for technical help.

References and Notes

- (1) Chuang, C. M.; Wu, M. C.; Huang, Y. C.; Cheng, K. C.; Lin, C. F.; Chen, Y. F.; Su, W. F. *Nanotechnology* **2006**, *17*, 4399.
- (2) Abargues, R.; Marques-Hueso, J.; Canet-Ferrer, J.; Pedrueza, E.; Valdes, J. L.; Jimenez, E.; Martinez-Pastor, J. P. *Nanotechnology* **2008**, *19*, 355308.
- (3) Bhuvana, T.; Kulkarni, G. U. *ACS Nano* **2008**, *2*, 457.
- (4) Ochiai, Y.; Manako, S.; Fujita, J. i.; Nomura, E. *J. Vacuum Sci. Technol. B* **1999**, *17*, 933.
- (5) Bogle, K. A.; Dhole, S. D.; Bhoraskar, V. N. *Nanotechnology* **2006**, *17*, 3204.
- (6) Mahapatra, S. K.; Bogle, K. A.; Dhole, S. D.; Bhoraskar, V. N. *Nanotechnology* **2007**, *18*, 135602.
- (7) Eilers, H.; Biswas, A.; Pounds, T. D.; Norton, M. G.; Elbahri, M. *J. Mater. Res.* **2006**, *21*, 2168.
- (8) Porel, S.; Singh, S.; Harsha, S. S.; Rao, D. N.; Radhakrishnan, T. P. *Chem. Mater.* **2005**, *17*, 9.
- (9) Deshmukh, R. D.; Composto, R. J. *Chem. Mater.* **2007**, *19*, 745.
- (10) Basak, D.; Karan, S.; Mallik, B. *Chem. Phys. Lett.* **2006**, *420*, 115.
- (11) Basak, D.; Karan, S.; Mallik, B. *Solid State Commun.* **2007**, *141*, 483.
- (12) Khan, M.; Oldhama, C.; Tuck, D. *Can. J. Chem.* **1981**, *59*, 2714.
- (13) Bhuvana, T.; Kulkarni, G. U. *Bull. Mater. Sci.* **2008**, *31*, 201.
- (14) Austin, M. D.; Zhang, W.; Ge, H.; Wasserman, D.; Lyon, S. A.; Chou, S. Y. *Nanotechnology* **2005**, *16*, 1058.
- (15) John, N. S.; Kulkarni, G. U. *J. Nanosci. Nanotechnol.* **2005**, *5*, 587.
- (16) Bhuvana, T.; Kulkarni, G. U. *Bull. Mater. Sci.* **2008**, *31*, 201–206.
- (17) Seah, M. P.; Briggs, D. *Practical Surface Analysis by Auger and X-ray Photoelectron Spectroscopy*, 2nd ed.; Wiley & Sons: Chichester, U.K., 1992.
- (18) Salz, D.; Lamber, R.; Wark, M.; Baalman, A.; Jaeger, N. *Phys. Chem. Chem. Phys.* **1999**, *1*, 4447.
- (19) Rao, C. N. R.; Thomas, P. J.; Kulkarni, G. U. *Nanocrystals: Synthesis, Properties and Applications*; Springer-Verlag: Berlin, 2007.
- (20) Agrawal, V. V.; Kulkarni, G. U.; Rao, C. N. R. *J. Phys. Chem. B* **2005**, *109*, 7300.
- (21) Farcau, C. A.; Astilean, S. *J. Optoelectron. Adv. Mater.* **2005**, *7*, 2721.
- (22) Subramaniam, C.; Sreeprasad, T. S.; Pradeep, T.; Pavan Kumar, G. V.; Narayana, C.; Yajima, T.; Sugawara, Y.; Tanaka, H.; Ogawa, T.; Chakrabarti, J. *Phys. Rev. Lett.* **2007**, *99*, 167404.
- (23) Zhang, J.; Fu, Y.; Chowdhury, M. H.; Lakowicz, J. R. *Nano Lett.* **2007**, *7*, 2101.
- (24) Ferrari, A. C.; Robertson, J. *Phys. Rev. B* **2000**, *61*, 14095.
- (25) Flouttard, J. L.; Akinnifesi, J.; Cambriil, E.; Despax, B. *J. Appl. Phys.* **1991**, *70*, 798.
- (26) Gelves, G. A.; Lin, B.; Sundararaj, U.; Haber, J. A. *Adv. Funct. Mater.* **2006**, *16*, 2423.

JP811062M